NEW APPROXIMATIONS FOR SORM: PART 2

By Yan-Gang Zhao[1] and Tetsuro Ono[2]

ABSTRACT: In the second-order reliability method, the Hessian matrix is used to construct a paraboloid approximation of the limit state surface and compute a second-order estimate of the failure probability. In this paper, a practical point-fitting second-order reliability approximation is proposed, by which the explicit second-order approximation of the performance function is obtained directly in standard normal space with neither the computation of Hessian matrix nor the computation of gradients of the function. Once the point-fitted performance function is obtained, the failure probability is estimated by the empirical second-order reliability index, which is generally simple and works well compared to other second-order reliability method formulas. For accurate computation of the failure probability, an IFFT method is proposed, from which the failure probability is obtained conveniently using the Inverse Fast Fourier Transformation. The proposed methods are investigated and their accuracy and efficiency are demonstrated using numerical examples.

INTRODUCTION

The ultimate goal in structural reliability analysis is to evaluate the probability content of part of an n-dimensional probability space. Difficulty in computing this probability has led to the development of various approximation methods (Bjerager 1991). Of interest here is the second-order reliability method (SORM), wherein the limit state surface is approximated by a paraboloid in a transformed standard normal space (Fiessler et al. 1979; Breitung 1984; Der Kiureghian et al. 1987, 1991; Tvedt 1988, 1990). There are two kinds of second-order reliability approximations: curvature-fitting SORM and point-fitting SORM.

In the curvature-fitting SORM, the approximated second-order limit state surface is defined by matching its principal curvatures to the principal curvatures of the limit state surface at the design point. The principal curvatures of the limit state surface are obtained as the eigenvalues of the rotational transformed second-order derivative matrix (Hessian matrix) of the performance function in standard normal space (Fiessler et al. 1979; Breitung 1984). For the paraboloid approximation, various formulas have been derived in closed form (Breitung 1984; Tvedt 1988; Koyluoglu and Nielsen 1994; Cai and Elishakoff 1994). These formulas generally work well for cases with large curvature radii and a small number of random variables (Zhao and Ono 1999). However, applying the curvature-fitting method in engineering requires the computation of the Hessian matrix, which can be prohibitively costly when the number of random variables is large and the performance function involves complicated numerical algorithms. Furthermore, the rotational transformation and eigenvalue analysis of the Hessian matrix are required and they are quite complicated for practicing engineers. To avoid the rotational transformation and eigenvalue analysis of the Hessian matrix, a simple approximation together with an empirical second-order reliability index has been proposed (Zhao and Ono 1998) that is simpler and more accurate than the previously mentioned formulas. However, the computation of the Hessian matrix is still required.

Difficulty in computing the Hessian matrix has led to the development of another type of SORM approximation, the point-fitting SORM method (Kiureghian et al. 1987, 1991), in which an efficient algorithm is derived in order to determine the principal curvatures without computing the Hessian matrix. The major principal axis of the limit state surface and the corresponding curvature are obtained in the course of obtaining the design point; the remaining principal axes and curvatures can be obtained in the order of decreasing absolute curvature, which coincides with the order of the importance of the principal curvatures in SORM analysis. Avoiding computation of the Hessian matrix is a promising advance in the application of SORM; however, some drawbacks exist in the application of this method. For example, the current point-fitting SORM uses certain gradient-based optimization algorithms, and computing the gradients of the limit state surface may also be prohibitively costly when the number of random variables is large and the performance function involves complicated numerical algorithms. In addition, because the current point-fitting SORM uses a point-fitted paraboloid in rotated standard normal space directly, the rotational transformation is still complicated and the application to general cases is difficult, suggesting that approximation of the limit state surface by a paraboloid at the design point may not be appropriate.

This paper presents an alternative point-fitting method for second-order reliability approximation, in which the performance function is directly point-fitted using a general form of the second-order polynomial standard, normal random variables in an iterative manner. The proposed method does not require computation of the Hessian matrix or the gradients of the performance function. Once the point-fitted limit state surface is obtained, the failure probability is conveniently obtained using the empirical second-order reliability index without any rotational transformation or eigenvalue analysis. Furthermore, as a accurate method, an IFFT method is proposed to compute the failure probability for the case of extremely small curvature radii or for the case in which the limit state surface cannot be approximated by a paraboloid at the design point. Numerical examples are used to confirm the efficiency and accuracy of the proposed methods.

SIMPLE POINT-FITTING SORM APPROXIMATION

In order to improve the current point-fitting SORM approximation (Kiureghian et al. 1987, 1991), consider the limit state surface in standard normal space expressed by a performance function $G(\mathbf{U})$. The present study defines the second-order surface approximation in terms of a set of fitting points on the limit state surface in the vicinity of the design point. These points, $2n + 1$ in number, are selected along the coordinate axes in standard normal space rather than in rotated normal space. Along each axis u_j, $j = 1, \ldots, n$, two points having the coordinates $(\mathbf{U}'^*, u_j^* - \delta)$ and $(\mathbf{U}'^*, u_j^* + \delta)$ are selected,

[1]Res. Assoc., Dept. of Arch., Nagoya Inst. of Technol., Gokiso-cho, Showa-ku, Nagoya 466-8555, Japan.

[2]Prof., Dept. of Arch., Nagoya Inst. of Technol., Gokiso-cho, Showa-ku, Nagoya, Japan.

Note. Associate Editor: Ross B. Corotis. Discussion open until June 1, 1999. Separate discussions should be submitted for the individual papers in this symposium. To extend the closing date one month, a written request must be filed with the ASCE Manager of Journals. The manuscript for this paper was submitted for review and possible publication on March 2, 1998. This paper is part of the ***Journal of Engineering Mechanics***, Vol. 125, No. 1, January, 1999. ©ASCE, ISSN 0733-9399/99/0001-0086–0093/$8.00 + $.50 per page. Paper No. 17820.

where $\mathbf{U}'^* = \{u_k^*, k = 1, \ldots, n \text{ except } j\}$ represents the coordinates of the design point along all the axes except the j-axis, and δ is a factor that represents the distance from the design point to the fitting point. The point-fitted performance function is expressed as a second-order polynomial of standard, normal random variables, including $2n + 1$ regression coefficients.

$$G'(\mathbf{U}) = a_0 + \sum_{j=1}^{n} \gamma_j u_j + \sum_{j=1}^{n} \lambda_j u_j^2 \tag{1}$$

where a_0, γ_j, and λ_j = $2n + 1$ regression coefficients.

Fitting the practical performance function $G(\mathbf{U})$ by $G'(\mathbf{U})$ at the fitting points described above, the regression coefficients a_0, γ_j, and λ_j can be determined from linear equations of a_0, γ_j, and λ_j obtained at each fitting point.

Computation of the Hessian matrix corresponding to $G(\mathbf{U})$ may be difficult, but the matrix corresponding to $G'(\mathbf{U})$ can be computed quite easily. Once the point-fitted performance function (1) is obtained, the Hessian matrix corresponding to (1) can be readily obtained as

$$\mathbf{B} = \frac{2}{|\nabla G'|} \begin{bmatrix} \boldsymbol{\lambda}_1 & \cdots & \mathbf{0} \\ \vdots & \ddots & \vdots \\ \mathbf{0} & \cdots & \boldsymbol{\lambda}_n \end{bmatrix} \tag{2}$$

where

$$|\nabla G'| = \sqrt{\sum_{j=1}^{n} (\gamma_j + 2\lambda_j u_j^*)^2} \tag{3}$$

The sum of the principal curvatures and the average principal curvature radius of the limit state surface at the design point $\mathbf{U}^*$ can be expressed (Zhao and Ono 1999) as

$$K_s = \sum_{j=1}^{n} b_{jj} - \boldsymbol{\alpha}^T \mathbf{B} \boldsymbol{\alpha} \tag{4}$$

$$R = \frac{n-1}{K_s} \tag{5}$$

where b_{jj}, $j = 1, \ldots, n - 1$ = diagonal elements of $\mathbf{B}$. $\boldsymbol{\alpha}$ = directional vector at design point $\mathbf{U}^*$.

Substituting (2) into (4), it follows that

$$K_s = \frac{2}{|\nabla G'|} \sum_{j=1}^{n} \lambda_j \left[1 - \frac{1}{|\nabla G'|^2} (\gamma_j + 2\lambda_j u_j^*)^2 \right] \tag{6}$$

With the aid of K_s and R expressed in (6) and (5), the failure probability corresponding to the point-fitted performance function can be obtained by substituting (5) into the following integration (Fiessler et al. 1979):

$$P_F = \int_0^\infty \Phi\left(\frac{t}{2R} - \beta_F\right) f_{\chi^2_{n-1}}(t)\, dt \tag{7}$$

where

$$f_{\chi^2_{n-1}}(t) = \frac{1}{\Gamma\left(\frac{n-1}{2}\right) 2^{(n-1)/2}} t^{(n-3)/2} \exp\left(-\frac{t}{2}\right) \tag{8}$$

or by substituting (5) and (6) into the following empirical second-order reliability index, which is an empirical closed-form solution for (7) (Zhao and Ono 1998):

$$\beta_S = -\Phi^{-1}\left[\Phi(-\beta_F)\left(1 + \frac{\phi(\beta_F)}{R\Phi(-\beta_F)}\right)^{-(n-1)/2[1+2K_s/10(1+2\beta_F)]}\right] \quad K_s \geq 0 \tag{9a}$$

$$\beta_S = \left(1 + \frac{2.5K_s}{2n - 5R + 25(23 - 5\beta_F)/R^2}\right)\beta_F + \frac{1}{2}K_s\left(1 + \frac{K_s}{40}\right) \quad K_s < 0 \tag{9b}$$

where K_s = sum of principal curvatures of limit state surface described in (6); R = average principal curvature radius described in (5); n = number of random variables; β_F = first-order reliability index; and β_S = second-order reliability index.

Although the procedure described above can be used to obtain the second-order reliability index conveniently, without computation of the Hessian matrix corresponding to $G(\mathbf{U})$ and without rotational transformation and eigenvalue analysis of the Hessian matrix corresponding to $G'(\mathbf{U})$, implementing this method requires the design point, which is not generally known beforehand. Computation of the design point for $G(\mathbf{U})$ requires the gradients of the limit state surface, which may also be prohibitively costly to compute when the number of random variables is large and the performance function involves complicated numerical algorithms. To avoid this problem, the design point will be obtained by the following iterative point-fitting procedure in standard normal space using the response surface approach (Bucher and Bourgund 1990; Rajashekhar and Ellingwood 1993).

1. Select an initial central point $\mathbf{U}_c$ in standard normal space (generally, the point corresponding to the mean value point in original space is recommended).
2. Select fitting points along the coordinate axes. Along each axis u_j, $j = 1, \ldots, n$, two points having the coordinates $(\mathbf{U}_c', u_{cj} - \delta)$ and $(\mathbf{U}_c', u_{cj} + \delta)$ are selected, where $(\mathbf{U}_c' = \{u_{ck}, k = 1, \ldots, n \text{ except } j\}$ represents the coordinates of the design point along all the axes except the j-axis, and δ is a factor which represents the distance from the central point to the fitting point.
3. Transform the fitting points to the original space using the Rosenblatt transformation, and fit the original performance function by the performance function approximation (1) at these points. The regression coefficients included in (1) can now be obtained.
4. For the point-fitted performance function (1), conduct FORM iteration and obtain the design point $\mathbf{U}^*$ corresponding to (1).
5. Substituting $\mathbf{U}^*$ for $\mathbf{U}_c$ in step 2, repeat steps 2–4 until convergence.
6. After obtaining the design point, the failure probability or the second-order reliability index can be obtained using (7) or (9).

According to the experience of the authors, this procedure generally converges after 3 to 6 iterations and is reasonably accurate, as shown in the ensuing sections.

ACCURATE COMPUTATION OF SECOND-ORDER RELIABILITY

Although the procedure described in the preceding section is simple, computation of the failure probability can be used only in the cases for which the limit state surface can be approximated by paraboloid, the assumption used in almost all of the current SORM methods. Generally, for the case of a relatively large curvature radius and a small number of random variables, the failure probability is not sensitive to the kind of limit state surfaces with a specified value of curvature radius, number of random variables, and first-order reliability index (Zhao and Ono 1997), and the formulas (7) and (9) work well. In the case of an extremely small curvature radius and a large number of random variables, and a limit state surface that cannot be approximated by a paraboloid, formulas (7) and (9) produce significant errors, and an alternate method is required for the accurate computation of failure probability. For this purpose, an Inverse Fast Fourier Transformation (IFFT) method, which uses the fact that the Probability Density Function (PDF) and the characteristic function of a random variable can be expressed as a pair of Fourier transformations (Lin 1967; Sakamoto and Mori 1995), is suggested.

$$Q(t) = \int_{-\infty}^{\infty} f(x)\exp(itx)\, dt \tag{10}$$

$$f(x) = \frac{1}{2\pi}\int_{-\infty}^{\infty} Q(t)\exp(-itx)\, dt \tag{11}$$

where $f(x)$ and $Q(t)$ are the PDF and characteristic function of a random variable x, respectively, and $i = \sqrt{-1}$.

The characteristic function corresponding to the point-fitted performance function (1) can be explicitly obtained as (Tvedt 1990)

$$Q(t) = \exp(ia_0 t)\prod_{j=1}^{n}\frac{\exp(-t^2\gamma_j^2/2(1 - 2it\lambda_j))}{\sqrt{1 - 2it\lambda_j}} \tag{12}$$

In particular, for the following performance function in the parabolic approximation (Breitung 1984; Tvedt 1983; Der Kiureghian et al. 1987, 1991; Hohenbichler et al. 1988; Koyluoglu and Nielsen 1994; Cai and Elishakoff 1994):

$$G(\mathbf{U}) = -(u_n - \beta_F) + \sum_{j=1}^{n-1}\lambda_j u_j^2 \tag{13}$$

the characteristic function is expressed as

$$Q(t) = \exp(i\beta_F t)\exp\left(-\frac{t^2}{2}\right)\prod_{j=1}^{n-1}\frac{1}{\sqrt{1 + 2it\lambda_j}} \tag{14}$$

Using the discrete values $Q(t_s)$, $s = 1, \ldots, N$, of (12) or (14) evenly distributed in the interval of $[t_1, t_N]$, where N = number of discrete data and $[t_1, t_N]$ can be selected by evaluating the effective range of $Q(t)$, the discrete values of inverse Fourier coefficients are readily obtained as F_r, $r = 1, \ldots, N$, using the IFFT, which has become a familiar engineering tool. According to the definition of discrete Fourier transformation and PDF, the discrete values of PDF can be obtained (see Appendix I) as

$$f(x_r) = \frac{t_N - t_1}{2\pi\sqrt{N}} F_r \exp(-it_1 x_r) \quad \text{for } x_r \geq 0 \tag{15}$$

where

$$x_r = \frac{2\pi(r - 1)}{t_N - t_1} \tag{16}$$

Because discrete values of $f(x)$ with only positive values of x are obtained, the failure probability for $Prob\{x < 0\}$ can be readily obtained by the numerical integration of the discrete values of $f(x)$.

$$P_f \approx 1 - \sum_{r=1}^{N-1}\frac{f(x_r) + f(x_{r+1})}{2}\Delta x \tag{17}$$

where

$$\Delta x = 2\pi/(t_N - t_1) \tag{18}$$

EXAMPLES AND INVESTIGATIONS

Example 1: Investigation on Convergence of Procedure

The object of the first example is to investigate the convergence of the proposed procedure. Consider the following simple performance function that includes only two random variables.

$$G(\mathbf{U}) = 80 - x_1 + x_2 \tag{19}$$

where x_1 = normal random variable with mean value of μ = 50 and standard deviation of σ = 25; and x_2 = lognormal random variable with mean value of μ = 80 and standard deviation of σ = 64. For comparison, the problem is first solved using gradient-based optimization algorithms, and the design point is obtained as (2.1334, −1.4000) in standard normal space with the first-order reliability index of β_F = 2.5518. Using differential geometry, the curvature radius is obtained as R = 3.7072 and the central point of the tangent circle is obtained as (5.2232, −3.4346) in standard normal space, as depicted by the thin solid line in Fig. 1. Using the integration method, the failure probability is obtained as 4.020×10^{-3} with the corresponding reliability index of β = 2.6504.

When the analysis is conducted using the proposed method, the initial central point is taken to be the point transformed from the mean value point, and the distance from the central

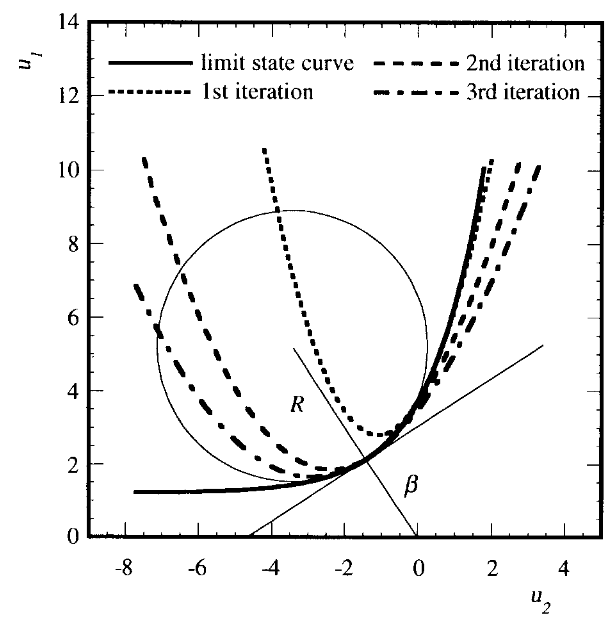

FIG. 1. Point-Fitted Limit State Surface for δ = 0.2

TABLE 1. Iterative Results for Example 1

Iteration (1)	Central point (2)	Point-fitted performance function (3)	Design point (4)	β_F (5)	R (6)	β_S (7)
No. 1	(0, 0.352)	$G'(\mathbf{U}) = 92.598 - 25u_1 + 42.513u_2 + 19.821u_2^2$	(2.802, −0.938)	2.9546	0.7395	3.2147
No. 2	(2.802, −0.938)	$G'(\mathbf{U}) = 90.715 - 25u_1 + 37.805u_2 + 8.004u_2^2$	(2.100, −1.450)	2.5520	2.8039	2.6739
No. 3	(2.100, −1.450)	$G'(\mathbf{U}) = 87.314 - 25u_1 + 32.081u_2 + 5.580u_2^2$	(2.150, −1.374)	2.5513	3.7459	2.6498
No. 4	(2.150, −1.374)	$G'(\mathbf{U}) = 87.924 - 25u_1 + 32.948u_2 + 5.887u_2^2$	(2.121, −1.418)	2.5516	3.6955	2.6510
Exact values		$G(\mathbf{U}) = 30 - 25u_1 + \mathrm{Exp}(0.7033u_2 + 4.1347)$	(2.133, −1.400)	2.5518	3.7072	2.6504

point to the fitting point is taken to be δ = 0.2. Convergence is obtained in four iterations with a tolerance of 0.0001. The results obtained in each iteration are listed in Table 1, in which column 1 is the number of iteration; column 2 is the central point for each iteration; columns 3 and 4 show the point-fitted performance functions and their corresponding design points, respectively, obtained in each iteration; and columns 5, 6, and 7 show the first-order reliability index β_F, the average principal curvature radius R, and the empirical reliability index β_S corresponding to the obtained point-fitted performance function, respectively. From Table 1 one can see that, although the results obtained in the first iteration are much different from the exact results, when convergence is reached (the fourth iteration), the design point is obtained as $\mathbf{U}^* = (2.121, -1.418)$ with corresponding first-order reliability index $\beta_F = 2.5516$, which is in good agreement with the exact results $\mathbf{U}^* = (2.133, -1.400)$ and $\beta_F = 2.5518$. Applying formulas (5), (6), and (9) to the point-fitted performance function obtained in the fourth iteration, the average curvature radius is obtained as 3.6955, and the failure probability is obtained as $P_F = 4.013 \times 10^{-3}$ with the corresponding reliability index of $\beta_S = 2.6510$, which are close to the exact results $R = 3.7072$, $P_F = 4.020 \times 10^{-3}$, $\beta = 2.6504$.

The point-fitted limit state surfaces obtained during each iteration are depicted in Fig. 1, in which the point-fitted limit state surface obtained in the fourth iteration is not depicted because it is almost identical to that obtained in the third iteration. Fig. 1 shows that the point-fitted limit state surface gradually approaches the original limit state surface at design point as the number of iterations increases. The tangent circle at the design point of the point-fitted limit state surface obtained in the fourth iteration is depicted by the thin dashed line. This circle is nearly invisible because it almost completely coincides with that of the original limit state surface. The central point of the circle is obtained as (5.2195, −3.4323), which is almost identical to the accurate central point (5.2232, −3.4346).

In order to investigate the effects of the fitting points, the previous problem is solved using different fitting points ranging from δ = 0.1 to δ = 2.0 with an interval of 0.1. All computations converged within six iterations, the first- and second-order reliability indices obtained with different δ are shown in Fig. 2, and the corresponding curvature radii are shown in Fig. 3. From Fig. 2, one can see that the first- and second-order reliability indices are only slightly affected by the fitting points, except when δ is very large. When δ is larger than 1.0, the first-order reliability index increased slightly with the increase of δ. In contrast, the second-order reliability index remains almost unchanged. This occurs because, in these cases, the curvature radius R also becomes large (see Fig. 3) and the modification effect of R becomes weak. As an example of large δ, the point-fitted second-order surface obtained with δ = 1.5 is depicted in Fig. 4, which shows that the tangent circle

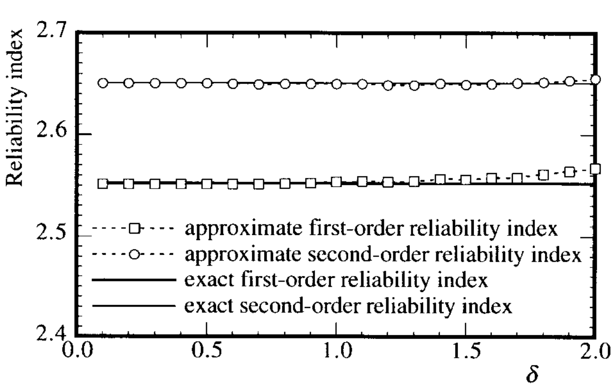

FIG. 2. Reliability Indices Affected by δ

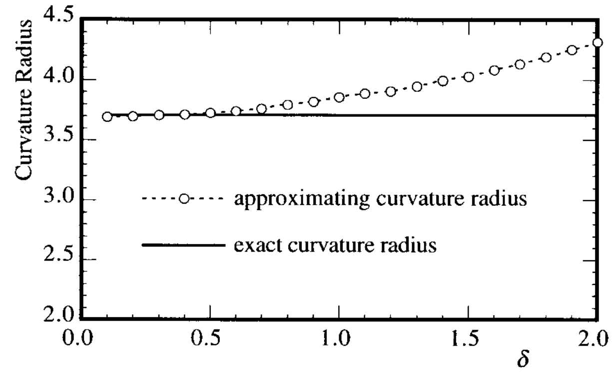

FIG. 3. Curvature Radius Affected by δ

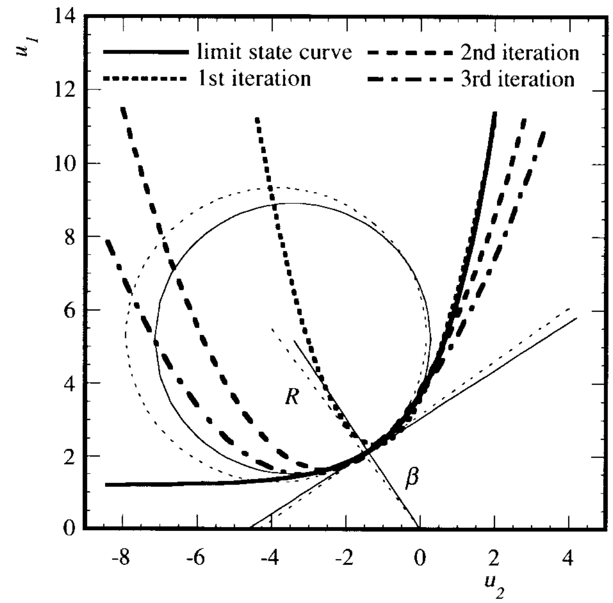

FIG. 4. Point-Fitted Limit State Surface for δ = 1.5

(depicted by a thin dashed line) of the point-fitted limit state surface does not closely approach that (depicted by a thin solid line) of the original limit state surface. The approximating curvature radius is obtained as $R = 4.0305$, which is very different when compared with the exact value $R = 3.7072$. The first- and second-order reliability index corresponding to the point-fitted limit state surface are obtained as $\beta_F = 2.5562$, $\beta_S = 2.6493$, respectively, which are still close to the exact values $\beta_F = 2.5518$, $\beta_S = 2.6504$.

Fig. 2 and Fig. 3 show that the value of δ should be between 0.1 and 0.5 for acceptable accuracy.

Example 2: Investigation on Efficiency of IFFT Method

Consider the following performance function in standardized space, which has been used as the fourth example by Der Kiureghian (1987). The relationships between the second-order reliability index and curvature radius, number of random variables, and first-order reliability index have been investigated by Zhao and Ono (1999).

$$G(\mathbf{U}) = \beta_F - u_n + \frac{1}{2}\sum_{j=1}^{n-1} jau_j^2 \tag{20}$$

The real and imaginary parts of the characteristic function are easily obtained as Fig. 5 and Fig. 6, respectively, for a = 0.01, 0.05, 0.1, 0.2, 0.3, 0.4, 0.5. As a by-product of the IFFT method, the corresponding PDFs in Fig. 7 are easily obtained, showing that the effective range of the PDF increases with the increase of a.

The sum of the principal curvatures of the limit state surface for (20) can be readily obtained as $K_s = an(n - 1)/2$, and the corresponding average curvature radius is obtained as $R = 2/na$. Using R, n, β_F as parameters, the failure probabilities obtained using the IFFT method proposed in this paper are listed in Table 2, with comparison of the results obtained using the empirical formula (9) and those using Monte-Carlo Simulation with 500,000 samples. The parameters β_F, n, R are listed in columns 1, 2, and 3, respectively; the reliability index β and the corresponding failure probability P_F obtained using the IFFT method are listed in columns 4 and 5, respectively; those obtained using Monte-Carlo simulation are listed in columns 6 and 7; and those obtained using formula (9) are listed in columns 8 and 9, respectively. From Table 1 one can see that when the curvature radius is small (the shaded rows of R = 3.3, 2.5, 2.0 with $\beta_F = 2$ and $n = 8$) or the number of random variables is large (the shaded rows of n = 24, 30 with $\beta_F = 2$ and $R = 5$), the errors in the empirical formula (9) become significant. However, there is very good agreement between the results obtained using the IFFT method and those obtained using Monte-Carlo simulation with any value of curvature radius R, number of random variables n and first-order reliability index β_F. In other words, the proposed IFFT method can be used to accurately compute the failure probability corresponding to quadratic performance functions in normal space.

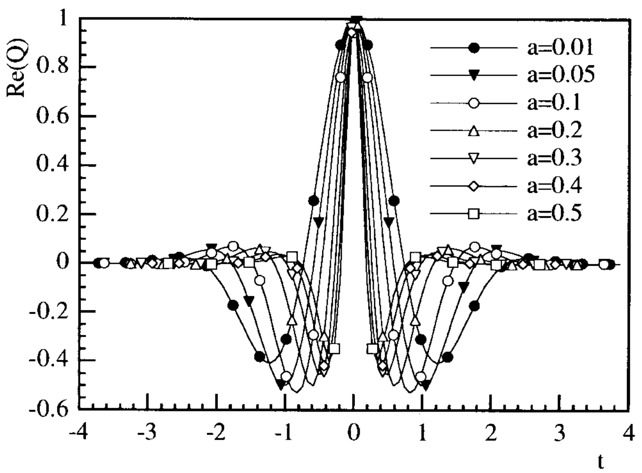

FIG. 5. Real Part of Characteristic Function for Example 2

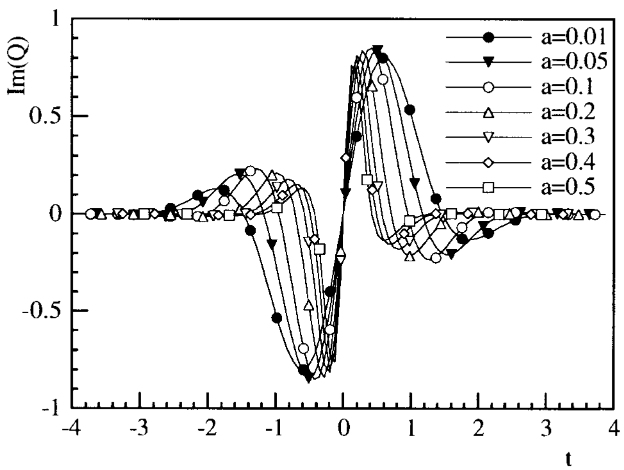

FIG. 6. Imaginary Part of Characteristic Function for Example 2

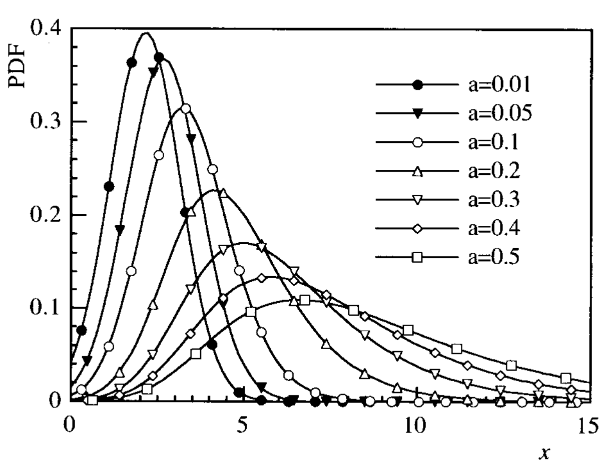

FIG. 7. PDF of Performance Function for Example 2

Example 3: Investigation on Effects of Noise

Consider the following performance functions that have been used as example 1 and example 2 by Der Kiureghian (1987):

$$G(\mathbf{X}) = x_1 + 2x_2 + 2x_3 + x_4 - 5x_5 - 5x_6 \tag{21}$$

$$G(\mathbf{X}) = x_1 + 2x_2 + 2x_3 + x_4 - 5x_5 - 5x_6 + 0.001 \sum_{j=1}^{6} \sin(1{,}000x_j) \tag{22}$$

Performance function (22) consists of (21) with artificial noise terms added. The approximating performance function obtained by the point-fitting approximation in this paper, the average principal curvature radius obtained using formula (5) and the second-order reliability index obtained using the empirical formula (9) are listed in Table 3. From Table 3, one can see that there are slight differences in the point-fitted performance function and the second-order reliability index, that is to say, the analysis results of the point-fitting approximation proposed in this paper are slightly affected by the noise.

Example 4: Comparison with Updating Method

Consider the two performance functions used by Hohenbichler and Rackwitz (1988), in which satisfactory results have been obtained by combining Breitung's formula with importance sampling:

$$G(\mathbf{X}) = C - \sum_{j=1}^{n} x_i \tag{23}$$

$$G(\mathbf{X}) = \sum_{j=1}^{n} x_i - C \tag{24}$$

where the x_i, $i = 1, \ldots, n$, are independently and identically exponentially distributed with parameter $\lambda = 1$. The exact result is known to be $P_F = F_{Ga}(C; n, \lambda)$ with F_{Ga} the Gamma (Erlang) distribution; (23) corresponds to the upper tail of F_{Ga} and (24) corresponds to the lower tail of F_{Ga}.

In order to compare the results obtained using the proposed method with those of Hohenbichler and Rackwitz's updating method (Hohenbichler and Rackwitz 1988; Fujita and Rackwitz 1988), the exact value of β and the number of random variables n are taken to be the same as those used by Hohenbichler and Rackwitz. The computational results using the proposed point-fitting method in this paper are listed in Table 4 for performance function (23) and in Table 5 for performance function (24). Columns 1, 2, and 3 are the parameters used by Hohenbichler (1988), where the values of $C(\beta, n)$ are provided for convenience of checking by readers. Columns 4, 5, 6, and 7 are the results given by Hohenbichler and Rackwitz's (1988), where β_S represents the Breitung's second-order reliability index and β_{SI} the updating reliability index using SORM combined with importance sampling, and the sign of the average curvature radius R has been corrected according to the definitions in this paper. Columns 8, 9, and 10 show the results obtained using the present method, where β_F is obtained using the point-fitting approximation, R is the average principal curvature radius obtained from the point-fitted performance function by formula (6) and (5), and β_S is the empirical second-order reliability index obtained using formula (9). From Table 4 and Table 5, one can see that the first-order

TABLE 2. Comparison of Results Obtained by IFFT and MCS for Example 1

Parameters			IFFT		Monte-Carlo		Eq. (9)	
β_F (1)	n (2)	R (3)	β (4)	P_F (5)	β (6)	P_F (7)	β (8)	P_F (9)
0.0	8	5.0	0.642	2.604×10^{-1}	0.643	2.603×10^{-1}	0.651	2.576×10^{-1}
0.4	8	5.0	1.019	1.541×10^{-1}	1.019	1.541×10^{-1}	1.005	1.574×10^{-1}
1.0	8	5.0	1.588	5.617×10^{-2}	1.589	5.603×10^{-2}	1.578	5.728×10^{-2}
1.8	8	5.0	2.352	9.338×10^{-3}	2.339	9.662×10^{-3}	2.354	9.291×10^{-3}
2.6	8	5.0	3.121	9.008×10^{-4}	3.123	8.941×10^{-4}	3.132	8.689×10^{-4}
2.0	2	5.0	2.083	1.862×10^{-2}	2.083	1.864×10^{-2}	2.081	1.871×10^{-2}
2.0	4	5.0	2.241	1.252×10^{-2}	2.240	1.255×10^{-2}	2.241	1.253×10^{-2}
2.0	6	5.0	2.394	8.331×10^{-3}	2.396	8.302×10^{-3}	2.396	8.287×10^{-3}
2.0	24	5.0	3.650	1.313×10^{-4}	3.648	1.320×10^{-4}	3.684	1.149×10^{-4}
2.0	30	5.0	4.032	2.764×10^{-5}	4.029	2.801×10^{-5}	4.085	2.206×10^{-5}
2.0	8	10.0	2.307	1.051×10^{-2}	2.308	1.051×10^{-2}	2.305	1.057×10^{-2}
2.0	8	5.0	2.544	5.482×10^{-3}	2.541	5.530×10^{-3}	2.548	5.414×10^{-3}
2.0	8	3.3	2.731	3.155×10^{-3}	2.726	3.210×10^{-3}	2.758	2.907×10^{-3}
2.0	8	2.5	2.885	1.958×10^{-3}	2.886	1.950×10^{-3}	2.930	1.694×10^{-3}
2.0	8	2.0	3.014	1.287×10^{-3}	3.026	1.240×10^{-3}	3.089	1.003×10^{-3}

TABLE 3. Effects of Noise for Example 3

Function (1)	Point-fitted performance function (2)	β_F (3)	R (4)	β_S (5)
Eq. (21)	$G'(u) = 273.08 + 11.91u_1 + 23.81u_2 + 23.81u_3 + 11.91u_4 - 54.82u_5 - 51.00u_6 + 0.584u_1^2 + 1.147u_2^2 + 1.147u_3^2 + 0.584u_4^2 - 17.91u_5^2 - 12.08u_6^2$	2.3483	−33.1704	2.2732
Eq. (22)	$G'(u) = 273.11 + 11.92u_1 + 23.81u_2 + 23.81u_3 + 11.92u_4 - 54.90u_5 - 50.94u_6 + 0.610u_1^2 + 1.147u_2^2 + 1.147u_3^2 + 0.610u_4^2 - 17.88u_5^2 - 12.11u_6^2$	2.3483	−33.2969	2.2734

TABLE 4. Computational Results in Example 4 for Performance Function (23)

Parameters			Hohenbichler and Rackwitz				Present Method		
Exact β (1)	n (2)	$C(\beta, n)$ (3)	β_F (4)	R (5)	β_S (6)	β_{SI} (7)	β_F (8)	R (9)	β_S (10)
2.327	2	6.4303	2.5413	−3.56	2.2419	2.3393	2.5417	−3.5567	2.3597
2.327	5	11.607	2.8890	−4.74	2.1008	2.2947	2.8896	−4.7420	2.3357
2.327	10	18.786	3.2391	−6.08	1.8994	2.3228	3.2397	−6.0792	2.3089
2.327	20	31.849	3.7088	−7.97	1.4845	2.3025	3.7094	−7.9758	2.3186
3.722	2	11.769	3.9177	−4.71	3.6542	3.7272	3.9208	−4.7141	3.7491
3.722	5	17.797	4.2545	−5.81	3.5460	3.6921	4.2574	−5.8165	3.7281
3.722	10	26.211	4.6007	−7.10	3.3998	3.7145	4.6036	−7.1015	3.7272
3.722	20	41.052	5.0685	−8.95	3.1260	3.7005	5.0714	−8.9554	3.7310
4.756	2	16.702	4.9416	−5.62	4.6987	4.7603	4.9441	−5.6205	4.7737
4.756	5	23.447	5.2697	−6.66	4.6045	4.7292	5.2721	−6.6584	4.7850
4.756	10	32.728	5.6124	−7.90	4.4797	4.7485	5.6149	−7.8979	4.7829
4.756	20	48.847	6.0785	−9.71	4.2539	4.7373	6.0809	−9.7132	4.8073

TABLE 5. Computational Results in Example 4 for Performance Function (24)

Parameters			Hohenbichler and Rackwitz				Present Method		
Exact β (1)	n (2)	$C(\beta, n)$ (3)	β_F (4)	R (5)	β_S (6)	β_{SI} (7)	β_F (8)	R (9)	β_S (10)
2.327	2	0.1484	2.0703	0.88	2.3305	2.3260	2.0712	0.8799	2.3420
2.327	5	1.2786	1.6837	1.96	2.2985	2.3292	1.6844	1.9620	2.3497
2.327	10	4.1291	1.3186	3.26	2.2225	2.3468	1.3192	3.2638	2.3362
2.327	20	11.080	0.8411	5.14	2.0474	2.3284	0.8417	5.1427	2.2967
3.722	2	0.0141	3.4692	0.57	3.7313	3.7185	3.4724	0.5748	3.7449
3.722	5	0.4433	3.0695	1.45	3.7225	3.7223	3.0705	1.4527	3.7709
3.722	10	2.1945	2.6921	2.64	3.6795	3.7410	2.6952	2.6440	3.7734
3.722	20	7.4348	2.2087	4.44	3.5667	3.7273	2.2116	4.4478	3.7435
4.756	2	0.0014	4.5138	0.44	4.7675	4.7533	4.5163	0.4466	4.7802
4.756	5	0.1686	4.1033	1.17	4.7636	4.7567	4.1059	1.1734	4.7884
4.756	10	1.2750	3.7178	2.25	4.7436	4.7772	3.7203	2.2580	4.7991
4.756	20	5.3594	3.2275	3.98	4.6621	4.7653	3.2300	3.9837	4.8186

reliability index β_F and the average principal curvature radius R obtained by the point-fitting approximation are in good agreements with those of Hohenbichler and Rackwitz's. Furthermore, although very simple, the empirical second-order reliability index β_S in column 10 agrees with the updating second-order reliability index β_{SI} in column 7. In addition, both of these reliability indices are significantly more accurate than Breitung's second-order reliability index β_S in column 6 and can be used as approximations of the exact reliability index listed in column 1.

CONCLUSIONS

For practical application of SORM, an alternative point-fitting approximation is proposed. The limit state surface is approximated by a point-fitted second-order surface in standard normal space that does not require computation of the Hessian matrix or the gradients of the performance function.

In order to compute the second-order reliability accurately, an IFFT method is proposed. This gives accurate failure probabilities corresponding to quadratic performance functions in standard normal space conveniently. As a by-product of the IFFT method, and if necessary, the PDF corresponding to the performance function can be easily obtained.

After obtaining the point-fitted performance function, the second-order reliability index is conveniently obtained using the empirical reliability index, which is generally reasonable. For the case of an extremely small curvature radius or the case when the limit state surface is difficult to be approximated by a parabolic surface, the IFFT method can be used to compute the failure probability accurately.

It should be noted that the method proposed in this paper can be used only for limit state surfaces having only one design point, a restriction that also applies to other FORM/SORM methods. Otherwise, local convergence may occur and error results may be yielded.

Another problem that needs to be mentioned is that, although the ranges of parameters R, n, and β_F for which the simple approximation and empirical reliability index are accurate are much larger than those of other SORM formulas, an understanding of these numerical ranges in detail is important because it can help us to judge when the IFFT method may be used. Further study in this area is needed.

APPENDIX I. DERIVATION OF (15) AND (16)

Corresponding to the Fourier transformation pair in (10) and (11), the pair of discrete Fourier transformation used in FFT and IFFT is defined as (Wolfram 1996)

$$Q_s = \frac{1}{\sqrt{N}} \sum_{r=1}^{N} F_r \exp\left[\frac{2\pi i(r-1)(s-1)}{N}\right] \tag{25}$$

$$F_r = \frac{1}{\sqrt{N}} \sum_{s=1}^{N} Q_s \exp\left[-\frac{2\pi i(r-1)(s-1)}{N}\right] \tag{26}$$

where N = number of discrete data, Q_s, $s = 1, \ldots, N$, = Fourier coefficients corresponding to F_r, $r = 1, \ldots, N$, or F_r, $r = 1, \ldots, N$, = inverse Fourier coefficients corresponding to Q_s, $s = 1, \ldots, N$.

For the discrete values $Q(t_s)$, $s = 1, \ldots, N$, of (12) or (14) evenly distributed in the interval of $[t_1, t_N]$, the discrete values of the PDF can be obtained as (27) from (11):

$$f(x_r) = \frac{1}{2\pi} \sum_{s=1}^{N} Q(t_s)\exp(-it_s x_r)\Delta t \tag{27}$$

where $\Delta t = (t_N - t_1)/N$.

Substituting $t_s = t_1 + \Delta t(s - 1)$ into (27), it follows that

$$f(x_r) = \frac{\Delta t}{2\pi} \exp(-it_1 x_r) \sum_{s=1}^{N} Q(t_s)\exp[-i\Delta t(s-1)x_r] \tag{28}$$

Using the following relationship:

$$x_r = x_1 + \Delta x(r - 1) \tag{29}$$

$$\Delta x = \frac{2\pi}{t_N - t_1} \tag{30}$$

and making $x_1 = 0$, one can obtain

$$x_r = \frac{2\pi(r-1)}{t_N - t_1} \tag{31}$$

Substituting (31) into (28), it follows that

$$f(x_r) = \frac{t_N - t_1}{2\pi N} \exp(-it_1 x_r) \sum_{s=1}^{N} Q(t_s)\exp\left[\frac{-i2\pi(s-1)(r-1)}{N}\right] \tag{32}$$

Comparing (31) with (26), it follows that:

$$f(x_r) = \frac{t_N - t_1}{2\pi\sqrt{N}} F_r \exp(-it_1 x_r) \quad \text{for } x_r \geq 0 \tag{33}$$

where F_r, $r = 1, \ldots, N$ = inverse Fourier coefficients for data $Q(t_s)$, $s = 1, \ldots, N$, they can be conveniently obtained from IFFT.

Because x_1 is made to be 0 here, only $f(x_r)$ for $x_r \geq 0$ can be obtained using (33).

As a reference, for discrete values $f(x_r)$, $r = 1, \ldots, N$, evenly distributed in the interval of $[x_1, x_N]$, the discrete values of the characteristic function can be obtained similarly as

$$Q(t_s) = \frac{x_N - x_1}{N} Q_s \exp(it_s x_1) \quad \text{for } t_s \geq 0 \tag{34}$$

where Q_s, $s = 1, \ldots, N$ = Fourier coefficients for data $f(x_r)$, $r = 1, \ldots, N$, they can be conveniently obtained from FFT.

ACKNOWLEDGMENTS

The writers wish to thank the reviewers of this paper for their critical comments and suggestions.

APPENDIX II. REFERENCES

Bjerager, P. (1991). ''Methods for structural reliability computation.'' *Reliability problems: General principles and applications in mechanics of solid and structures*, F. Casciati, ed., Springer, New York, 89–136.

Breitung, K. (1984). ''Asymptotic approximation for multi-normal integrals.'' *J. Engrg. Mech.*, ASCE, 110(3), 357–366.

Bucher, C. G., and Bourgund, U. (1990). ''A fast and efficient response surface approach for structural reliability problems.'' *Structural Safety*, 7, 57–66.

Cai, G. Q., and Elishakoff, I. (1994). ''Refined second-order reliability analysis.'' *Structural Safety*, 14, 267–276.

Der Kiureghian, A., Lin, H. Z., and Hwang, S. J. (1987). ''Second-order reliability approximations.'' *J. Engrg. Mech.*, ASCE, 113(8), 1208–1225.

Der Kiureghian, A., and De Stefano, M. (1991). ''Efficient algorithm for second-order reliability analysis.'' *J. Engrg. Mech.*, ASCE, 117(12), 2904–2923.

Fiessler, B., Neumann, H.-J., and Rackwitz, R. (1979). ''Quadratic limit states in structural reliability.'' *J. Engrg. Mech.*, ASCE, 105(4), 661–676.

Hohenbichler, M., and Rackwitz, R. (1988). ''Improvement of second-order reliability estimates by importance sampling.'' *J. Engrg. Mech.*, ASCE, 114(12), 2195–2199.

Johnson, N. I., and Kotz, S. (1970). *Distribution in statistics, continuous univariate distributions-2*, Houghton Mifflin, Boston.

Koyluoglu, H. U., and Nielsen, S. R. K. (1994). ''New approximations for SORM integrals.'' *Structural Safety*, 13, 235–246.

Lin, Y. K. (1967). *Probabilistic theory of structural dynamics*. Krieger, Malabar, Fla.

Rajashekhar, M. R., and Ellingwood, B. R. (1993). ''A new look at the response surface approach for reliability analysis.'' *Structural Safety*, 12, 205–220.

Sakamoto, J., and Mori, Y. (1995). ''Probability analysis method by fast Fourier transform: Accuracy, efficiency, and applicability of the method.'' *Proc., Asian-Pacific Symp. on Struct. Reliability and its Applications*, Tokyo, 32–39.

Tvedt, L. (1983). ''Two second-order approximations to the failure probability.'' *Veritas Rep. RDIV/20-004083*, Det norske Veritas, Oslo.

Tvedt, L. (1988). ''Second-order reliability by an exact integral.'' *Proc., 2nd IFIP Working Conf. on Reliability and Optimization on Struct. Sys.*, P. Thoft-Christensen, ed., Springer, New York, 377–384.

Tvedt, L. (1990). ''Distribution of quadratic forms in normal space—application to structural reliability.'' *J. Engrg. Mech.*, ASCE, 116(6), 1183–1197.

Wolfram, S. (1996). *Mathematica, a system for doing mathematics by computer*, Second edition, Addison-Wesley, Tokyo, 657–660 (in Japanese).

Zhao, Y. G., and Ono, T. (1997). ''An empirical reliability index based on SORM.'' *Proc., 7th Int. Conf. on Struct. Safety and Reliability*, Kyoto, Japan.

Zhao, Y. G., and Ono, T. (1999). ''New Approximations for SORM: Part 1.'' *J. Engrg. Mech.*, ASCE, 125(1), 79–85.

APPENDIX III. NOTATION

The following symbols are used in this paper:

a_0 = regression coefficient in point-fitted performance function;
$\mathbf{B}$ = scaled second-order derivatives of $G(\mathbf{U})$ at $\mathbf{U}^*$, i.e., Hessian matrix;
b_{jj} = diagonal elements of $\mathbf{B}$;
F_r = inverse Fourier transformation coefficients obtained by IFFT;
$f(x)$ = probability density function with argument x;
G = performance function;
G' = point-fitted performance function;
i = imaginary unit, $i = \sqrt{-1}$;
K_s = sum of principal curvatures of limit state surface;
N = number of data used in IFFT method;
n = number of random variables;
P_F = failure probability;
Q_s = Fourier transformation coefficients obtained by FFT;
$Q(t)$ = characteristic function of random variable;
R = average principal curvature radius;
$\mathbf{U}$ = standard normal random variables;
$\mathbf{U}_c$ = central point;
$\mathbf{U}^*$ = design point in u-space;
$\boldsymbol{\alpha}$ = directional vector at design point in u-space;
β_F = first-order reliability index;
β_S = second-order reliability index;
$\Phi(x)$ = standard normal probability distribution with argument x;
$\phi(x)$ = standard normal density distribution with argument x;
γ_j = regression coefficients in point-fitted performance function; and
λ_j = regression coefficients in point-fitted performance function.